PROGRESS IN AMORPHOUS SILICON SOLAR CELLS PRODUCED BY REACTIVE SPUTTERING

T. D. MOUSTAKAS
Corporate Research Laboratory
Exxon Research and Engineering Company
Clinton Township
Route 22 East
Annandale, New Jersey 08801

Summary

In this paper we review the photovoltaic properties of reactively sputtered amorphous silicon and show that efficient PIN solar cells can be fabricated by the method of sputtering. The photovoltaic properties of the intrinsic films correlate with their structural and compositional inhomogeneities. Hydrogen incorporation and small levels of phosphorus and boron impurities also affect the photovoltaic properties through reduction of residual dangling bond related defects and modification of their occupation. The optical and transport properties of the doped P and N-films were found to depend sensitively on the amount of hydrogen and boron or phosphorus incorporation into the films as well as on their degree of crystallinity. Combination of the best intrinsic and doped films leads to PIN solar cell structures generating J_{SC} of 13 mA/cm^2 and V_{OC} of between 0.85 to 0.95 volts. The efficiency of these devices, 5 to 6%, is limited by the low FF, typically about 50%. As a further test to the potential of this technology we fabricated efficient tandem solar cell structures and tested device design concepts, such as the incorporation of optically reflective back contacts.

1. INTRODUCTION

Of the two plasma methods for depositing hydrogenated amorphous silicon the glow discharge decomposition of silane has attracted considerably more attention, and this led to the fabrication of solar cells with efficiencies up to 10% (1). This breakthrough resulted partly through progress in the thin film growth process (2) and partly through improvements in the device design (3).

The alternative technology of reactive sputtering has attracted much less attention, primarily because early work suggested that sputtered amorphous silicon solar cells are inferior to those produced by the glow discharge process (4,5). In addition there is a wide-spread belief that sputtering is an unsuitable technology for surface sensitive devices (6).

In this paper we show that the properties of both the intrinsic and doped sputtered amorphous silicon films can be optimized to lead to solar cell structures with high efficiencies. Correlations between the photovoltaic properties and structural and compositional inhomogeneities, hydrogen content, and small levels of phosphorus and boron impurities in the intrinsic films have been studied. The doped films were optimized for maximum transparency and conductivity, through the variation of the amount of hydrogen and phosphorus or boron incorporation. The role of degree of crystallinity in the transport and optical properties of the doped films

was also investigated. The photovoltaic potential of the sputtered amorphous silicon films was assessed through the fabrication and evaluation of single and tandem PIN solar cell structures. Device design concepts such as the incorporation of optically reflective back contacts have been tested.

2. EXPERIMENTAL METHODS

The deposition system used in this study has been described in more detail in another paper (7). Here we briefly review only the most important features and emphasize primarily the methods of device fabrication. The deposition system has stainless steel walls, held at ground potential and electrically insulated cathode and anode assemblies. The water cooled target, a polycrystalline silicon disk 5" in diameter and 1/4" thick, is supplied with an RF power at a frequency 13.56 MHz. The anode assembly, 26" in diameter, is held 2" below the target and can be grounded, floated or supplied with RF or DC electrical bias.

The main deposition variables were the partial pressures of argon and hydrogen, the concentrations of PH_3 and B_2H_6 in the sputtering gas and the target and substrate bias voltages.

The investigated devices have the configurations: substrate/N-I/Pt (or Pd), substrate/N-I-P/ITO, and substrate/P-I-N/ITO. All active layers (N,I,P) were deposited in the same deposition chamber but not sequentially. The deposition system was scrupulously cleaned between N and I or P and I layers.

The films were characterized for evidence of crystallinity by x-ray diffraction, and for hydrogen incorporation and bonding by infrared absorption spectroscopy. The optical absorption coefficient was calculated from optical transmission measurements. The conductivity was measured on samples deposited on quartz substrates.

Each device was characterized by measuring its I-V characteristics with a calibrated Xenon simulator and the spectral dependence of the collection efficiency (8). The short circuit current was calculated by integrating the spectral response with the (AM)1 solar spectrum (9).

3. EXPERIMENTAL RESULTS AND DISCUSSION

3.1 Photovoltaic properties of intrinsic films

The photovoltaic properties of the intrinsic films were found to depend sensitively on deposition parameters which affect their structural and compositional inhomogeneities as well as the amount of incorporated hydrogen and traces of phosphorus and boron impurities. Some of these properties have been described in a number of recent papers (10-17). In this article we present a comprehensive summary of these results.

3.1.1 Effect of Structural and compositional inhomogeneities

Structural studies on glow discharge and sputtered amorphous silicon films (2,18) revealed that the deposition of these films proceeds via nucleation and growth of island structures (average lateral dimensions $\sim$100Å). The coalescence of these islands if imperfect, leads to columnar morphology in subsequent growth. Another type of structural inhomogeneities are microvoids of about 10Å in diameter, which have been observed in small angle scattering experiments (19). The existence of such structural inhomogeneities in the silicon network are also expected to lead to compositional inhomogeneities upon alloying the material with hydrogen or other impurities. Such types of inhomogeneities have been observed

through NMR, neutron scattering and infrared vibrational studies (20-22). It has been shown that these type of structural and compositional inhomogeneities in sputtered material are controlled by charged particle bombardment during the growth of the film (7,18,23). Deposition parameters which affect charged particle bombardment are the pressure of sputtering gas, the target voltage and the substrate bias.

Structural and compositional inhomogeneities may affect the photovoltaic properties of the films in a variety of ways. An example of this is the introduction of dangling bond related defect, which control recombination, and another is the introduction of structural and compositional disorder, which affects the extend of the band tails and therefore influences carrier transport and optical properties (24). To illustrate this correlation we show in Figs. 1 and 2 the effect of argon pressure and target voltage respectively on the photovoltaic properties of the sputtered films.

Fig. 1 shows the I-V characteristics of a number of Schottky barrier structures having the configuration SS/N-I-Pd. The I-layer in these devices was deposited at 5, 10, 20 and 30 mTorr of argon and constant all other deposition parameters. Note that the films produced at argon pressures of 20 and 30 mTorr have poorer photovoltaic properties than those produced at 5 and 10 mTorr of argon. This result correlates fairly well with structural studies (7,18), which reveal no evidence of columnar morphology for films produced at low argon pressures and strong evidence of columnar morphology for films produced at high argon pressures.

Fig. 2 shows the spectral dependence of the collection efficiency for two series of Schottky barrier structures (SS/N-I-Pt) produced with the target voltage of the only variable. In one series the induced DC target voltage was maintained at -800 volts and in the other at -1000 volts. In each series the flow rates of H_2/Ar were varied from 0.1 to 0.2. Note that these spectra fall into two distinct groups, which correlate with the target voltage but not with the hydrogen content in the discharge. For the -800V samples the collection efficiency peaks at 450nm, while for the -1000V samples it peaks at 500nm. The fact that the collection efficiency of the devices produced at each target voltage is independent of hydrogen content is significant, and suggests that the observed effect is not related to changes of the optoelectronic properties of the films due to the hydrogen incorporation. Therefore, the shift of the peak of the collection efficiency towards the red part of the spectrum, as the target voltage (power in the discharge) increases, suggests that the electronic quality of the films improves with the power in the discharge. This is contrary to the findings (2) that the quality of the glow discharge amorphous silicon films improves with decreasing power in the discharge. The improvement of the sputtered material with the power in the discharge is believed to have originated in more perfect coalescence of the island structure due to additional bombardment by charged particles (11).

The substrate bias was found to have a significant effect on compositional inhomogeneities (bonding configuration of hydrogen) and on the optical properties of the films (7,10,23). The effect of such inhomogeneities on carrier transport and recombination and their combined effect on the photovoltaic properties is under current study.

3.1.2 Effect of hydrogen content

It has been shown (12,13) that the density of states in the middle of the gap depends exponentially on the partial pressure of hydrogen in the discharge and that these states control the electron-hole recombination in amorphous silicon solar cells. Since the states in the middle of the gap

determine both the width of the space charge region and electron hole recombination (diffusion length of the minority carriers), one would expect that the photovoltaic properties of the amorphous silicon films should improve with the amount of incorporated hydrogen. However, besides reducing the density of states in the middle of the gap, hydrogen incorporation also affects the optical properties of the films. As an illustration we show in Figure 3 the optical absorption constant vs. photon energy of the films whose collection efficiencies are shown in Figure 2. Note that the optical gap (26) of the films produced at -1000 volts has increased from 1.71 to 1.84 eV. This dual role of hydrogen in reducing the states in the middle of the gap while simultaneously increasing the optical gap is an unfortunate trade-off, since the photovoltaic properties of a semiconductor depend both on its ability to absorb a significant fraction of the solar spectrum and its ability to collect the photogenerated electron-hole pairs. This trade-off explains the insensitivity of the collection efficiency to hydrogen content. According to the data of Figures 2 and 3 films having optical gaps between 1.71 to 1.84 eV generate the same J_{sc}. Therefore, the larger gap material has a better photovoltaic potential because it produces the same current and higher open circuit voltage (14).

3.1.3 Effects of Phosphorus and boron impurities

The effects of phosphorus and boron impurities on the photovoltaic properties of the intrinsic films were investigated by studying N-I-Pt Schottky barrier structures, whose I-layer was contaminated intentionally with small amounts of PH_3 or B_2H_6 or both (16,17). The effects of phosphorus contamination and boron compensation of the intrinsic layer are shown in Fig. 4. Samples 295, 384 and 385 were prepared under the same deposition conditions for the I-layer but with progressively longer evacuation times between N and I depositions (20 min, 2h and 24h). Sample 387 was prepared under the same pumping mode as sample 385 but the I-layer was intentionally doped by adding 0.1 ppm of B_2H_6 in the sputtering gas. The improvement in the collection efficiency with evacuation time between N and I depositions is related to the decrease in phosphorus incorporation into the I-layer. The additional improvement in Sample 387 is related to boron compensation of residual phosphorus donors in the I-layer.

The effect of increasing the boron concentration in the I-layer beyond the value of total compensation is shown in Fig. 5. This figure shows the spectral dependence of the collection efficiency for three Schottky barrier structures having the configuration glass/SnO_2/N-I-Pt. The N-layer in all three samples was deposited in a different deposition run and the sputtering chamber was thoroughly cleaned before the deposition of the I-layer. The amount of B_2H_6 in the discharge during the growth of the I-layers was 0.02, 0.2 and 0.4 ppm for the samples 406, 478 and 468 respectively. Note that as the level of B_2H_6 in the discharge increased to more than about 0.1 ppm the quantum efficiency for blue-green light decreases significantly. However, the blue-green response is restored when the devices are illuminated from the glass side.

These results can be understood along the lines of recent doping models of amorphous silicon (27,28), which predict that substitutional doping can only occur in the presence of localized gap states and that the density and nature of these localized states is influenced by the position of the Fermi level. Overcompensation by boron renders the I-layer P-type and moves the major barrier to the I-N interface. Therefore, in such devices, illumination from the N-side gives better photovoltaic performance.

3.2 Properties of doped films

Phosphorus and boron doped films have been fabricated either in amorphous or microcrystalline form. We find that the critical parameter for the transition from the one regime to the other is the relative concentrations of hydrogen to argon in the discharge. Films produced under conditions of $H_2/Ar < 1$ were found by x-rays to be amorphous and those produced under $H_2/Ar >> 1$ were found to be partially crystallized. The mechanisms of crystallization and details of structural, optical and transport properties of both amorphous and microcrystalline films are discussed elsewhere (29,30). Here we give only a brief summary of the results which affect the performance of solar cell structures.

Fig. 6 shows the optical absorption constant vs photon energy for one amorphous boron doped film and two microcrystalline films one doped with phosphorus and the other with boron. The amorphous film was deposited at 325°C with H_2 + Ar = 5mT (H_2/Ar = 0.4) and 0.2 at.% of B_2H_6 in the discharge. The microcrystalline films were also deposited at 325°C with H_2 + Ar = 40 mT (H_2/Ar = 10) and 0.2 at.% of B_2H_6 or PH_3 in the discharge respectively. Note that for the same level of doping the microcrystalline films are far more transparent in the visible part of the spectrum than the amorphous films.

Besides the difference in their optical properties these films have also different transport properties. The amorphous film has room temperature conductivity of $10^{-4}\Omega^{-1}cm^{-1}$ and conductivity activation energy of 0.27eV. The microcrystalline films have room temperature conductivities of between 1 to 10 $\Omega^{-1}cm^{-1}$ and the weak temperature dependence suggests degenerate conduction. The microcrystalline doped films are therefore more suitable for photovoltaic applications than amorphous doped films.

3.3 Solar cells

Solar cell structures were fabricated in the configurations: SS/N-I-P/ITO and SS/P-I-N/ITO. The deposition chamber was cleaned between N and I or P and I depositions to minimize the phosphorus and boron contamination effects, which were discussed previously. Since boron contamination was found to be far more severe than phosphorus contamination the most efficient cells were fabricated with the first configuration. Besides contamination effects, the optical and transport properties of the doped layers were found to have a significant effect on the device performance. For example, devices fabricated with amorphous P and N layers were reported to have an efficiency of about 4% (31). This performance can be improved significantly upon using microcrystalline P and N layers, due to their high conductivity and reduced optical absorption in the visible spectral region. As an example, we show in Figs. 7 and 8 the I-V characteristics and the spectral dependence of the collection efficiency of one such device. The I-layer of this device was produced at 5 mTorr of Ar + H_2 (H_2/Ar = 0.18), at target voltage of -800 volts and deposition temperature of 325°C. The P and N layers were deposited under the conditions described in section 3.2. This solar cell structure generates a J_{SC} of $13^{mA}/cm^2$ and V_{OC} of 0.86 Volts. The efficiency of this device, 5.5%, is limited by the low FF of 0.49. In the following we discuss the factors which limit the efficiency of these devices and suggests methods for further improvments.

The low value of the FF is partly due to the degradation of the N-I interface which results from the need to clean the chamber between N and I depositions. It has been shown in another paper (16) that the FF increases from 0.49 to 0.57 as the evacuation time between N and I depositions decreases from 24h to 20 min. Also studies of the wavelength dependence of the FF were accounted for in terms of surface recombination at the N-I

interface (32). Therefore, the low value of the FF is not inherent, to the sputtered devices. Sequential deposition of all layers in interlocked, dedicated sputtering chambers should lead to FF's equivalent to those found in cells prepared by the glow discharge decomposition of silane process (1).

The J_{SC} can be increased by further improvements in the film's structural and compositional homogeneity and by improvements in the device design. As an example, we show in Fig. 9 how the incorporation of back reflective contacts can improve the red portion of the spectrum. The two devices have the configurations: substrate/N-I-P/ITO. In the one device the substrate is SS and in the other is SS/Ag/TiO_2. The TiO_2 layer, approximately 30 Å thick, acts to prevent diffusion of silver into the amorphous silicon. Incorporation of highly transparent a-SiC heterocontact should result in significant improvement in the blue part of the spectrum (1). Therefore, upon implementation of these device design concepts the J_{SC} should approach the values of cells produced by the glow discharge process.

The V_{OC} value is also expected to increase upon minimizing cross contamination and improving the device design. Values of V_{OC} as high as 0.95 Volts have already been observed in devices having the configuration: SS/N-I-P/ITO.

To further test the potential of this technology we fabricated tandem solar cell structures having the configuration: SS/N-I-P-N-I-P/ITO. The I-layers in both solar cells was made under the same conditions, and their thickness was not adjusted for current matching. The P and N layers were microcrystalline. The I-V characteristics of this device, shown in Fig. 10, suggests good junction characteristics. In particular, the tunneling between the microcrystalline P and N layers appears to be satisfactory. These initial results suggest that high efficiency tandem cells can be fabricated by the method of sputtering if a smaller gap material, made for example from α-SiGe alloys, is used as a back solar cells.

4. CONCLUSIONS

The studies presented in this paper showed that the properties of both the intrinsic and doped sputtered amorphous silicon films can be optimized to produce high efficiency solar cells.

The photovoltaic properties of the intrinsic films were found to depend sensitively on structural and compositional inhomogeneities, amount of incorporated hydrogen and low levels of dopant impurities.

Conditions for deposition of both amorphous as well as microcrystalline phosphorus and boron doped films have been identified. These films were characterized through studies of their optical and transport properties and the superiority of the microcrystalline films for photovoltaic applications has been demonstrated.

The combination of the best intrinsic and doped films led to the fabrication of P-I-N solar cell structures with efficiency 5.5%. We showed that this efficiency can be improved even further by depositing the three layers in sequential dedicated chambers and by implementing device design concepts such as back reflective contacts and highly transparent a-SiC front contacts. Finally, the photovoltaic potential of this technology was demonstrated through the fabrication of efficient tandem solar cell structures.

ACKNOWLEDGMENTS

The author is indebted to B. Abeles, G. Cody, P. Maruska, A. Rose, T. Tiedje and C. Wronski for a number of technical discussions and to R. Friedman and M. Hicks for technical assistance. The work was partially supported by the U.S. Department of Energy through a Solar Energy Research Institute Contract (Contract #ZB-3-02166-01).

REFERENCES

1. Catalano, A., D'Aiello, R. V., Dresner, J., Faughnan, B., Firester, A., Kane, J., Schade, H., Smith, Z. E., Swartz, G., and Triano, A. (1982). IEEE Photovoltaic Spec. Conf. 16, 1421.
2. Knights, J. C., and Lujan, R. A. (1979). Appl. Phys. Lett. 35, 244.
3. Hamakawa, Y., Fujimoto, K., Okuda, K., Kashima, Y., Nonomura, S., and Okamoto, H. (1983) Appl. Phys. Lett. 43, 644.
4. Thompson, M. J., Allison, J., Al-Kaisi, M. M., and Thomas, I. P. (1978). Rev. Phys. Appl. 13, 625.
5. Victorovitch, P., Jousse, D., Chenevas-Paule, A., and Lieuz-Rocherz, L. (1979). Rev. Phys. Appl. 14, 204.
6. Amick, J. A., Schnable, G. L., Vossan, J. L. (1977). J. Vac. Sci. Technol. 14, 1053.
7. Moustakas, T. D. (1982). Sol. Energy Mater. 8, 187.
8. Wronski, C. R., Abeles, B., and Cody G. D. (1980) Solar Cells, 2, 245.
9. Bird, R., (1981). Terrestrial Solar Spectral Standards and Data Sets, SERI/TR-642-1149.
10. Moustakas, T. D. (1983). "Photovoltaics for Solar Energy Applications II", D. Adler, Ed., Proc. SPIE 407, 56.
11. Moustakas T. D., and Maruska, H. P. (1983) Appl. Phys. Lett. 43.
12. Tiedje, T., Moustakas, T. D. and Cebulka, J. M. (1981). Phys. Rev. B 23, 5634.
13. Moustakas, T. D., Wronski, C. R. and Tiedje, T. (1981). Appl. Phys. Lett. 39, 721.
14. Morel, D. L., and Moustakas, T. D. (1981). Appl. Phys. Lett. 39, 612.
15. Moustakas, T. D., Wronski, C. R., and Morel, D. L. (1980). J. Non-Crystall. Solids, 35-36, 719.
16. Moustakas, T. D., Friedman, R., Weinberger B. R. (1982). Appl Phys. Lett. 40, 587.
17. Moustakas, T. D., Maruska, H. P., Friedman, R., and Hicks M. (1983). Appl. Phys. Lett. 43, 368.
18. Ross, R. C., and Messier, R. (1981). J. Appl. Phys. 52, 5329.
19. D'Andonio, P., and Konnert, J. H. (1979). Phys. Rev. Lett. 43, 1161.
20. Jeffrey, F. R., Lowry, M. E., Garcia, M. L. Barnes, R. G., and Torgeson, D. E. (1981) In "Tetrahedrally Bonded Amorphous Semiconductors" (R. A. Street, D. K. Biegelsen, and J. C. Knights, eds) p. 83, Am. Inst. Phys. New York.
21. Postol, T. A., Falco, C. M., Campuirth, R. T., Schuller, I. K. and Yelon W. B. (1980) Phys. Rev. Lett. 45, 648.
22. Freeman, E. C., and Paul, W. (1978). Phys. Rev. B 18, 4288.
23. Moustakas, T. D. (1984). In "Hydrogenated Amorphous Silicon/Semiconductors and Semimetals", Ed. by J. Pankove (Academic Press, New York).
24. Cody, G. D., Tiedje, T., Abeles, B., Brooks, B., and Goldstein, Y. (1981). Phys. Rev. Lett. 47, 1480.
25. Movchan, B. A., and Demshishin, A. V. (1969). Fiz. Met Metalloved, 28 653.
26. The
B(h
27. Adl
28. Str
29. Mou
be
30. Mou
31. Mou
32. Mar

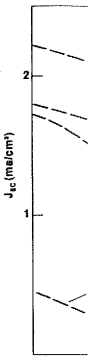

Fi

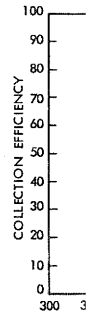

Figu

26. The optical gap, Eg., is defined by the relation: $(ahv)^{1/2} = B(hv-Eg)$.
27. Adler, D., (1978). Phys. Rev. Lett. 41, 1755.
28. Street, R. A. (1982). Phys. Rev. Lett. 49, 1187.
29. Moustakas, T. D., Maruska, H. P., Friedman R., and Hicks, M. (To be published).
30. Moustakas, T. D., and Maruska, H. P. (To be published).
31. Moustakas, T. D., and Friedman, R. (1982). Appl. Phys. Lett. 40, 515.
32. Maruska, H. P., and Moustakas, T. D. (To be published).

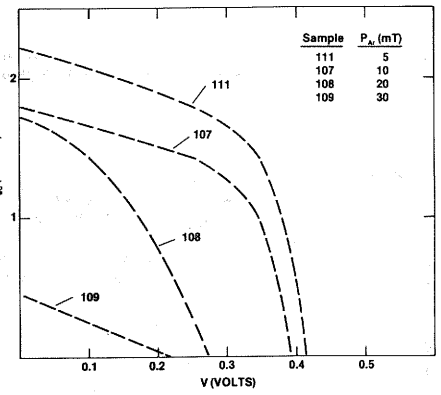

Figure 1. I-V Characteristics of N-I-Pd Schottky Barrier structures.

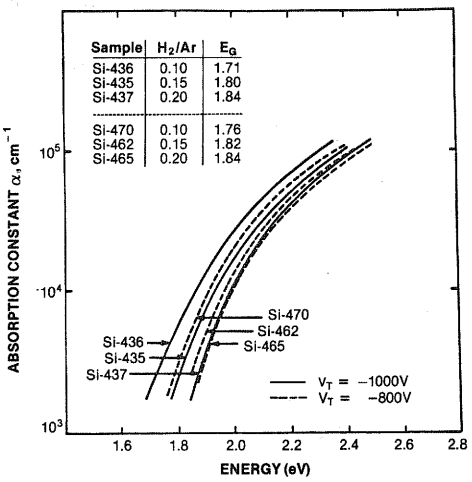

Figure 3. Optical Absorption Constant vs. Photon Energy for Two Series of Films Produced under Target Voltage of −1000 V and −800 V

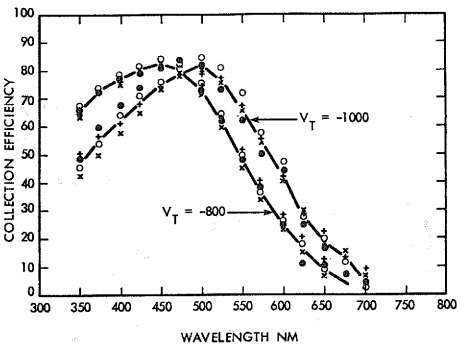

Figure 2. Spectral Dependence of the Collection Efficiency of two Series of N-I-Pt Devices, Made at Indicated Voltages.

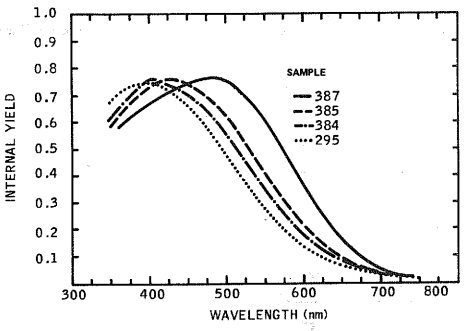

Figure 4. Effect of Phosphorus Contamination and Boron Compensation on the Collection Efficiency of N-I-Pt Devices

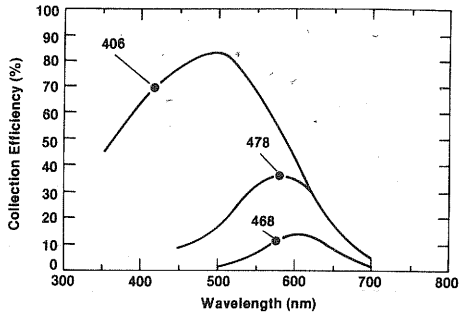

Figure 5. Effect of Boron Compensation on Spectral Dependence of Collection Efficiency of N-I-Pt Devices.

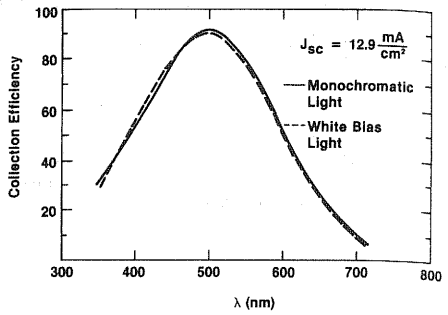

Figure 8. Spectral Dependence of the Collection Efficiency of the Device Shown in Figure 7.

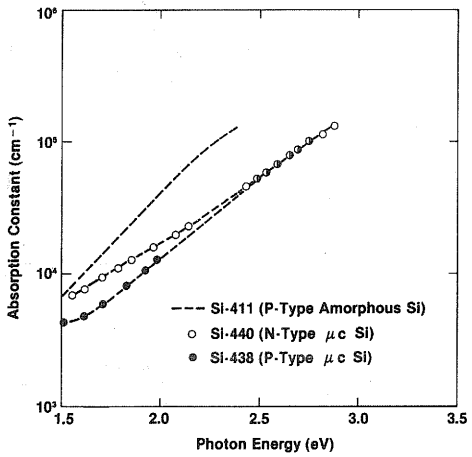

Figure 6. Optical Absorption Constant vs. Photon Energy for Amorphous and Microcrystalline Silicon Doped Films

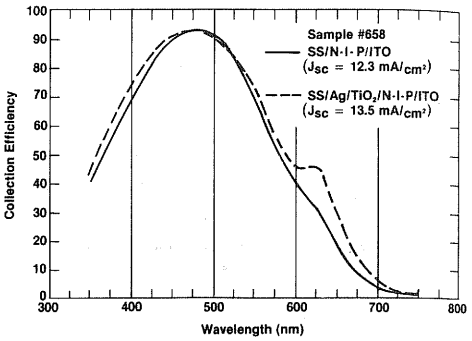

Figure 9. The Effect of Substrate Reflectivity on the Spectral Dependence of the Collection Efficiency of Sputtered Solar Cells

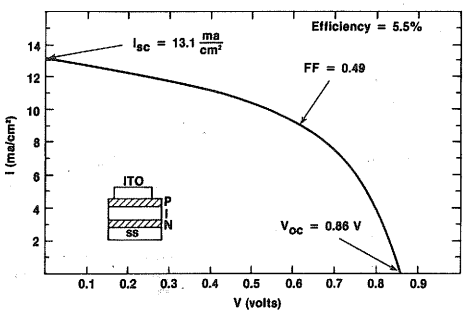

Figure 7. I-V Characteristics of a Sputtered SS/NIP/ITO Solar Cell Structure.

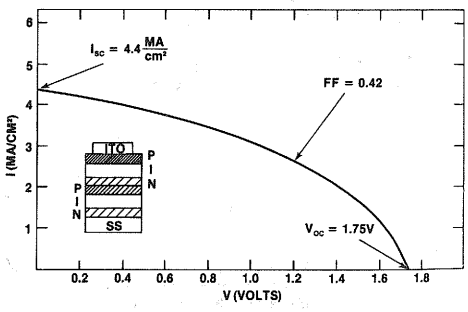

Figure 10. I-V Characteristics of a Sputtered SS/NIP NIP/ITO Solar Cell Structure